J. Biochem. 2009;145(2)193–198
doi:10.1093/jb/mvn156

The 1.9 Å X-Ray Structure of Egg-white Lysozyme from Taiwanese Soft-Shelled Turtle (*Trionyx Sinensis* Wiegmann) Exhibits Structural Differences from the Standard Chicken-Type Lysozyme

Jaruwan Siritapetawee[1], Sompong Thammasirirak[2], Robert C. Robinson[3] and Jirundon Yuvaniyama[4,*]

[1]College of Medicine and Public Health, Ubon Rajathanee University, Ubon Ratchathani 34190; [2]Department of Biochemistry, Faculty of Science, Khon Kaen University, Khon Kaen 40002, Thailand; [3]Institute of Molecular and Cell Biology, Proteos, Singapore 138673; and [4]Department of Biochemistry and Center for Excellence in Protein Structure and Function, Faculty of Science, Mahidol University, Bangkok 10400, Thailand

Received September 12, 2008; accepted November 10, 2008; published online November 23, 2008

Lysozyme from Taiwanese soft-shelled turtle (SSTLB) has been purified from turtle egg white and crystallized. The crystals diffract X-rays beyond 2 Å resolution and belong to the orthorhombic $P2_12_12_1$ space group containing one molecule per asymmetric unit. The structure was elucidated using pheasant egg-white lysozyme as the molecular replacement search template. The overall structure of SSTLB is very similar to that of hen egg-white lysozyme (HEWL). Nevertheless, Pro104 in the substrate subsite A and other amino acids in the substrate subsites E and F differ from those of HEWL. These substitutions result in local conformational differences in the substrate binding sites of the two enzymes, effecting substrate binding and transglycosylation efficiency, translating into differing ranges of products.

Key words: crystal structure, lysozyme, soft-shelled turtle, transglycosylation, X-ray crystallography.

Abbreviations: HEWL, hen egg-white lysozyme; JSSTL, Japanese soft-shelled turtle lysozyme; NAG, *N*-acetylglucosamine; NAM, *N*-acetylmuramic acid; PDB, Protein Data Bank; PEWL, pheasant egg-white lysozyme; RMSD, root-mean-square deviation; SDS–PAGE, sodium dodecyl sulfate-polyacrylamide gel electrophoresis; SSTLA and SSTLB, Taiwanese soft-shelled turtle lysozymes A and B.

INTRODUCTION

Lysozyme (EC 3.2.1.17) is an enzyme found in egg white, tears and other secretions. This enzyme provides protection against certain bacterial invasions by cleaving the β-linkage between *N*-acetylmuramic acid (NAM) and *N*-acetylglucosamine (NAG) of the bacterial cell-wall peptidoglycan layer, leading to bacterial cell lysis. This property of lysozyme has led to its utilization in the pharmaceutical and food industries. Lysozyme is used in hemorrhoid treatment (Siduol) and as an additive to cow's milk making it resemble more closely the properties of human breast milk (*1*). In addition to hydrolysis activity, lysozyme also catalyses transglycosylation (*2*). The molecular mechanism of this highly efficient process remains enigmatic. It is known that amino acids in the substrate-binding subsites E and F affect the efficiency of tranglycosylation (*3*). Substrates are thought to bind to 'Asn46-wall' and 'Arg114-wall' of the E and F binding subsites, respectively (*4*) during the transglycosylation process. Thus, information on 3D structures of subsites E and F is needed to further understand the reaction mechanism and specificity of transglycosylation in lysozyme catalysis.

Lysozymes from various organisms have earlier been classified into three different types, namely chicken-type or C-type (*5–7*), goose-type or G-type (*8–10*), and T4 phage-type or Phage-type (*11*, *12*) based on their sources and molecular properties. The sequence, structure and function of hen egg-white lysozyme (HEWL) have been extensively studied making this C-type lysozyme the most widely used standard for lysozyme studies. The pheasant egg-white lysozyme (PEWL, *Phasianus colchicus*) is also classified as C-type based on its overall structural features (*13*). Recently, a novel member of the lysozyme family, invertebrate-type or I-type lysozyme, has been identified. This discovery created much interest because of differences in the primary structure compared with the previously known lysozymes, namely the different number of cysteine residues and the lack of conservation of the second catalytic amino acid (the active aspartate) (*14*).

Although the crystal structures and activities of many types of lysozyme have been studied, information concerning reptile lysozymes is less abundant. Lysozymes from egg white of tortoises and turtles were among the first reptilian enzymes purified since 1977 (*15*). Shortly after, a crystal structure of tortoise egg white lysozyme at 6 Å resolution was reported (*16*). The study of amino-acid sequence and activity of Japanese soft-shelled turtle lysozyme (JSSTL) was the first lysozyme from a reptilian source to be characterized in detail (*17*). Compared with

*To whom correspondence should be addressed. Tel: +66-2-201-5603, Fax: +66-2-354-7174, E-mail: scjyv@mahidol.ac.th

HEWL, different amino acids are present in all six substrate-binding sites of JSSTL. At subsites E and F, the amino acids His35, Tyr46, Arg48 and Tyr116 (corresponding to Phe34, Arg45, Thr47 and Arg 114 of HEWL, respectively) are thought to contribute to the reduction of rate constant for glycosidic cleavage and the increase in free energy of binding at both subsites (*17*). Novel lysozymes from common Thai turtles, Asiatic soft-shelled turtle (*Amyda cartilagenea*), soft-shelled turtle (*Trionyx sinensis*) and green sea turtle (*Chelonia mydas*) were recently purified and characterized (*18*). *T. sinensis* possesses at least two C-type lysozymes (SSTLA and SSTLB), which differ in activity, although the basis of this difference at primary structure level is unknown. Here, we have purified SSTLB, a 14.8-kDa single peptide chain of 131 amino-acid residues with 100% identical sequence to that of JSSTL, and elucidated its tertiary structure by X-ray analysis. The structure reveals the first indication of the basis of specificity and provides a valuable framework for understanding the evolution of reptilian lysozymes.

EXPERIMENTAL PROCEDURES

Purification and Crystallization—Freshly laid eggs from soft-shelled turtles (*T. sinensis* Wiegmann) were purchased from a local breeding farm. SSTLB was purified following the published protocol (*18*). Briefly, the egg white was diluted with two volumes of 0.03 M phosphate buffer, pH 7.0 and centrifuged at $12,000 \times g$ for 15 min. The supernatant was subjected to isoelectric precipitation at pH 4.0 or 7.0 by using 1 M HCl or 1 M NaOH for pH adjustment, and then centrifuged at $12,000 \times g$ for 30 min. The clarified supernatant was applied to a CM-Toyopearl 650 M cation exchange column (1.3×90 cm) equilibrated with 0.03 M phosphate buffer, pH 7.0. The enzyme was eluted with a linear gradient of NaCl from 0 to 0.25 M in 0.03 M phosphate buffer, at a flow rate of 15 ml h^{-1}. The eluted enzyme was dialysed against distilled water. The molecular weight of the purified SSTLB was determined on 12.5% gel SDS–PAGE as described by Laemmli (*19*), by using the low molecular weight calibration kit for SDS electrophoresis (GE Healthcare Life Sciences) as a standard protein set. The enzyme concentration was determined by the BCA™ Protein Assay Kit (Pierce) standardized against bovine serum albumin.

Orthorhombic crystals were obtained from $(2 + 2\,\mu l)$ protein drops using 20 mg ml^{-1} purified SSTLB and 30% (w/v) polyethyleneglycol 8000, 0.2 M ammonium sulfate, 0.1 M sodium cacodylate, pH 6.5 as a precipitant in sitting-drop vapour-diffusion experiments at 18°C. For data collection, the crystals were vitrified in cold nitrogen stream (–170°C) after a 10–15 s transfer to a cryoprotectant solution, 30% (w/v) polyethylenelycol 8000 and 0.2 M ammonium sulfate in 0.1 M sodium cacodylate, pH 6.5 containing 20% (v/v) glycerol.

Data Collection—A crystal $(440 \times 80 \times 20\,\mu m^3)$ of SSTLB diffracted X-rays beyond 2.0 Å resolution on a Rigaku/MSC R-AXIS IV^{++} detector using an RU-H3R rotating anode generator running at 50 kV and 100 mA, with Osmic Blue confocal focusing mirrors and a 0.3 mm collimator. Diffraction data were recorded over an 85° rotation of the crystal around the phi axis with an oscillation width of 1° per image. The integrated intensities were obtained using the program *CrystalClear*/*D***TREK* (*20*).

Structure Determination and Refinement—Initial phases of the SSTLB structure were determined by the molecular replacement technique with the *AMoRe* program (*21*) in the CCP4 package (*22*), using a probe model of the pheasant egg-white lysozyme (PDB code 1GHL) (*13*). Restrained refinement was performed in the program *REFMAC5* (*23*). Manual rebuilding of the model was achieved with the graphic program O (*24*) based on $2|F_o|-|F_c|$ and $|F_o|-|F_c|$ electron density maps. Stereochemistry of the final model was assessed with the program *PROCHECK* (*25*). Amino-acid sequences were aligned with *CLUSTAL W* (*26*) and displayed with *ESPript* (*27*) using BLOSUM62 score with cut-offs of 0.2 global score and 0.5 diff score. Figures containing structural representations were generated with the program *MOLMOL* (*28*).

RESULTS AND DISCUSSION

Structure Determination and Analysis—X-ray diffraction data from an SSTLB crystal were collected with statistics shown in Table 1. The V_M value of 2.57 $Å^3\,Da^{-1}$ falls within the normal range observed for protein crystals (*29*), and suggests that there is one molecule per asymmetric unit. The crystal structure of SSTLB was initially phased with the molecular replacement technique using PEWL as a template because of its 70% identity with SSTLB. The search produced an *R*-factor of 42.4% and 60.6% correlation on amplitudes at 3 Å resolution after the initial rigid-body fitting. Iterative model rebuilding and refinement resulted in the final *R*-factor of 20.7% at 1.9 Å resolution with 1,136 atoms in the model.

Table 1 also provides statistical information of the structure refinement. Analysis of the main-chain torsion angles shows that 88.7% of the non-glycine residues are

Table 1. **Data collection and refinement statistics.**

Parameters	SSTLB
Unit cell length (Å)	$a = 37.8$, $b = 55.6$, $c = 72.2$
Unit cell volume ($Å^3$)	151,536
Resolution range[a] (Å)	33.46–1.9 (1.97–1.90)
Completeness[a] (%)	99.4 (95.1)
No. of observed reflections	82,161
No. of unique reflections	12,477
R_{merge} (%)[a]	4.6 (21.4)
Refinement resolution range (Å)	17.2–1.9
No. of protein atoms	1,032
No. of water molecules	99
No. of sulfate ions	1
RMSD bond lengths (Å)	0.014
RMSD bond angles (°)	1.327
R-factor (%)	20.7
R_{free} (%)	23.2
Average B factor for all atom ($Å^2$)	21.15

[a]Values in parentheses belong to the data in the outermost shell.

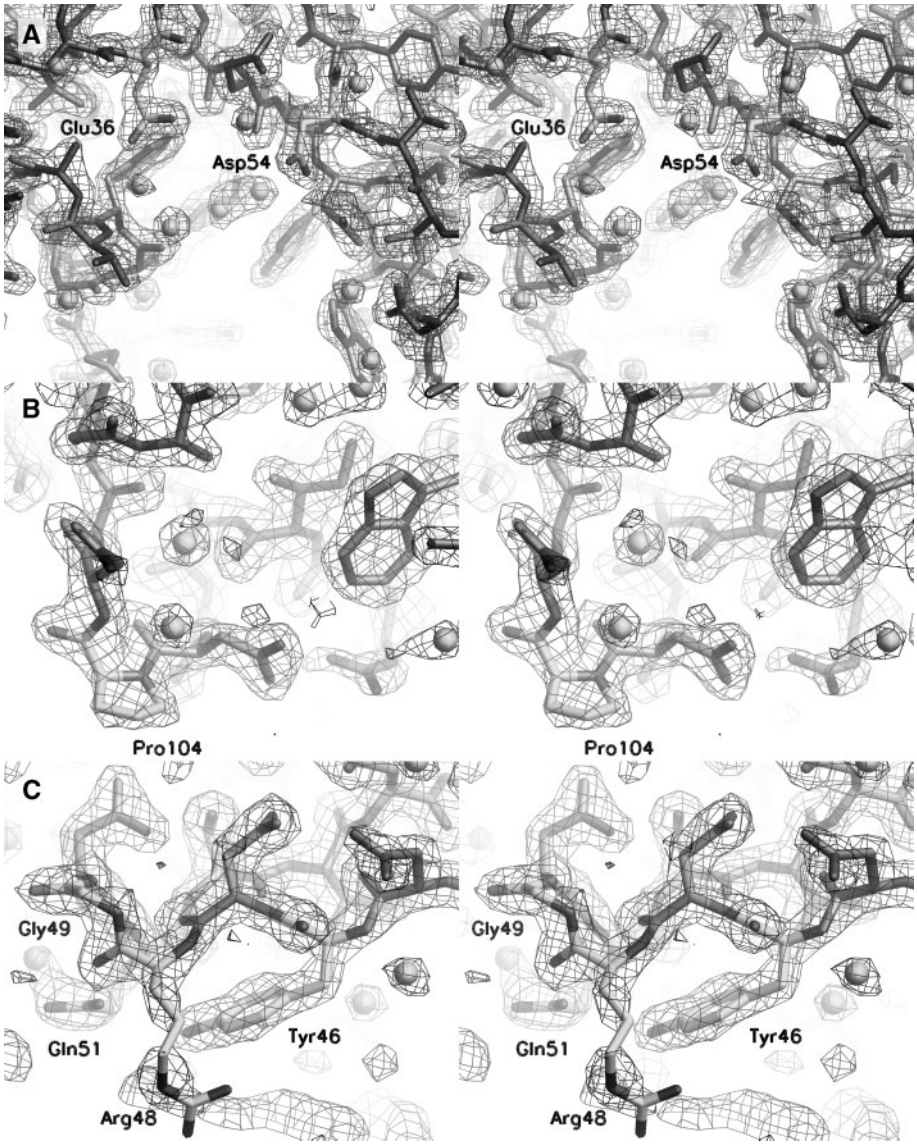

Fig. 1. **Stereo views of SSTLB electron density around (A) the active site, (B) Pro104 and (C) Gly49.** The electron density ($2|F_o|-|F_c|$) map is calculated at 1.9 Å resolution and contoured at 1.25σ. Tight-binding water molecules are depicted as spheres. The active-site residues Asp54 and Glu36, as well as key residues that differ from HEWL and PEWL are drawn with white carbon atoms and labelled.

located in the most favoured regions of the Ramachandran plot, and the remaining 11.3% are in the additionally allowed regions. The electron density map calculated at 1.9 Å resolution is shown in Fig. 1 around the active site, as well as the vicinities of Pro104 and Gly49, respectively. Coordinates and structure factors of SSTLB have been deposited in the Protein Data Bank (PDB code 2GV0).

Overall Structure of SSTLB—SSTLB adopts the standard HEWL fold, containing two sub-domains separated by the active-site cleft as shown in Fig. 2. The active-site residues Glu36 and Asp54 lie in a water-filled cleft at substrate-binding subsites C and D (Fig. 1A). This solvated region may allow the substrate to diffuse into the active site of SSTLB in a similar fashion to other lysozymes (*30*, *31*). One of the subdomains is almost entirely comprised of β-sheet structure (encompassing residues 1–4 and 39–62). The second sub-domain is mainly composed of α-helical structure (residues 6–36, 91–116 and 123–126). The two sub-domains are linked by a helix (residues 83–85). SSTLB has four disulfide bridges formed by pairs of cysteine residues (7:129), (31:117), (66:82) and (78:96) (Fig. 2A). These disulfide bridges are equivalent to those found in HEWL, PEWL and JSSTL (*17*, *32*) (Fig. 3). These data support the notion that the four disulfide bridges are critical to structural integrity of this group of lysozymes. Hill *et al*. (*33*) have shown that the reduction of one of the four disulfide bridges (6:127) in HEWL creates a flexible C-terminus and in turn exposes ubiquitination sites (Lys1/Lys13), leading to degradation of the lysozyme.

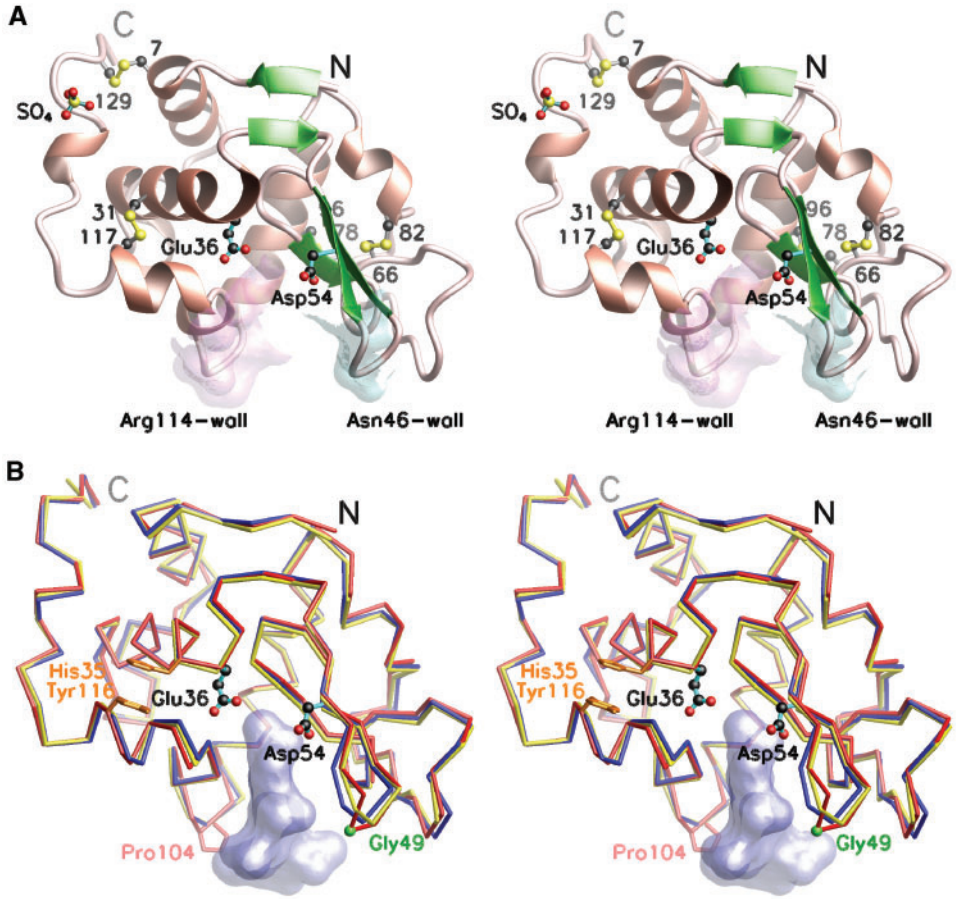

Fig. 2. **Stereo views of lysozyme structures.** (A) Ribbon diagram showing the backbone structure of SSTLB. (B) Comparison of lysozyme structures. Active-site residues Glu36 and Asp54 of SSTLB are drawn as ball-and-stick model with cyan bonds and are labelled as are the termini. (A) The α-helix structures are shown in pink helices and the β-sheet structures in green arrows. SSTLB has four disulfide bridges (depicted in yellow) formed by the pairs of cysteine residues (7:129), (31:117), (66:82) and (78:96). The sulfate ion found in the structure is also shown. The 'Arg114-wall' and the 'Asn46-wall' of substrate binding subsites E and F, named after the HEWL numbering, are referred to the surfaces outlined by His35, Glu36, Ala112 and Tyr116 (magenta), and residues 46–51 (cyan), respectively. (B) Superposition of the C_α-traces of SSTLB (red) with HEWL (blue) and PEWL (yellow) shows similarity of the overall structures among the three lysozymes. The inserted residue Gly49 of SSTLB is represented by a green sphere. Slight dislocation of the helix formed by residues 110–117 may be contributed by π–π stacking interaction between side chains of His35 and Tyr116, which are drawn with orange bonds. $(NAG)_3$ from the structure of HEWL (PDB code 1HEW) has been superimposed and drawn as light blue semitransparent surface to indicate substrate-binding subsites A–C. Pro104 of SSTLB drawn with red bonds would clash with the substrate $(NAG)_3$ if it were present in the SSTLB structure in this binding orientation. This suggests that a slightly different binding mode would be adopted resulting in different substrate recognition.

Structural Comparison—Comparison of the primary structures between SSTLB and HEWL, PEWL or JSSTL (Fig. 3), reveals high sequence identity (67%, 70% or 100%, respectively). SSTLB, JSSTL and PEWL have an extra Gly residue at the N-terminus in comparison with HEWL. The inserted Gly residue arises from an unusual proteolytic processing of prelysozyme between X-Gly rather than the more typical Gly–Lys (*17*, *34*).

Superposition of the main-chain structures of SSTLB, HEWL and PEWL is shown in Fig. 2B. All three structures are highly similar as characterized by RMSD over all C_α atoms of 0.44, 0.62 and 0.69 Å for the pair-wise comparison of HEWL:PEWL, SSTLB:PEWL and SSTLB:HEWL, respectively. These values suggest SSTLB is the outlying structure within this group. Despite the similarity in the overall tertiary structures of these three enzymes, three major disparities are notable (Fig. 2B).

First, the presence of Pro104 in SSTLB instead of a glycine as found in HEWL and PEWL provides an alternate backbone route for the turn in which these helix-breaking residues lie (Figs 1B, 2B and 3). The side chain of this proline also extends into the substrate binding site, suggesting there might be a slightly different substrate recognition. A previous study comparing the activities of two lysozymes that only differ at this position (either glycine or arginine) has demonstrated that this residue at subsites A–C affects the pattern of reaction products between the two enzymes (*17*).

The second difference occurs as small dislocation of a helix (residues 110–117, Fig. 2B). This displaced

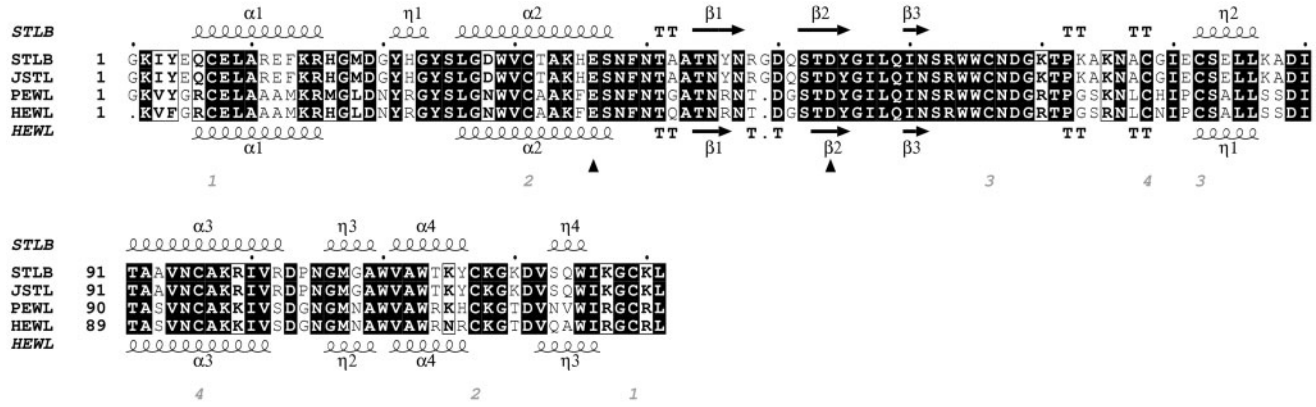

Fig. 3. **Amino-acid sequence comparison of SSTLB, JSSTL, PEWL and HEWL.** The sequences of SSTLB and JSSTL are denoted as STLB and JSTL, respectively. Secondary structures and sequence numbering marks (dots) depicted above and below the alignment are of SSTLB and HEWL, respectively. Squiggles (α), squiggles (η), arrows, or TT represent secondary structure elements: α-helices, 3_{10}-helices, β-strands or strict β-turns, respectively. Four pairs of the conserved Cys residues involved in disulfide bonds in all four lysozymes are indicated by italicized numbers below the alignment. The active-site residues, corresponding to Glu36 and Asp54 of SSTLB, are indicated with solid triangles.

structure appears to be stabilized by the *pi–pi* interaction between His35 and Tyr116 that are part of the 'Arg114-wall' of subsites E and F (Fig. 2). These residues correspond to Phe35 and His115 of PEWL, and Phe34 and Arg114 of HEWL, respectively (Fig. 3). Amino-acid substitutions on the 'Arg114-wall' of subsites E and F in duck egg-white lysozyme (Phe34 to Tyr and Asn37 to Ser, equivalent to His35 and Asn38 of SSTLB) cause a reduction of transglycosylation rate (*35*). Mutation of Arg114 to His of HEWL (corresponding to Tyr116 of SSTLB) results in the decreases of not only the binding free energy for subsites E and F but also the rate constant of transglycosylation (*36*). Similarly, Kawamura *et al*. have reported that Asn37 (Asn38 of SSTLB) is involved both in substrate binding and transglycosylation activities (*37*). Hence, the non-conserved amino acids and resulting small dislocation of the helix on the 'Arg114-wall' of subsites E and F of SSTLB may be expected to affect substrate binding at this site and possibly its transglycosylation activity.

The final difference occurs in a structurally variable loop that comprises the 'Asn46-wall' of subsites E and F (Fig. 2). Here, residues Tyr46, Arg48 and Gln51 (Fig. 1C) correspond to arginine, threonine and glycine, respectively, in both HEWL and PEWL (Fig. 3). Furthermore, SSTLB possesses an extra glycine at position 49 (Figs 1C and 3) as compared with HEWL and PEWL. Together, these amino-acid differences provide a distinct pattern of interactions and ultimately a different loop structure. Again, substrate binding may be affected by the altered surface properties and the distinctive loop conformation.

Although all three enzymes exhibit different crystal packing, the greater similarity in both primary and tertiary structures between HEWL and PEWL suggests that the structural divergence of SSTLB is amino-acid derived. JSSTL shares 100% sequence identity to SSTLB and demonstrates delayed substrate degradation and altered product pattern in comparison with HEWL (*17*). The structural variation arising from amino-acid differences in subsites A–C as well as both 'Asn46-wall' and 'Arg114-wall' of subsites E and F is likely responsible for this diversity in substrate binding and transglycosylation kinetics. This work, therefore, represents a basis on which to understand SSTLB specificity. The structures of SSTLB/substrate complexes and the precise roles of the critical amino acids identified here will be further investigated in future work.

ACKNOWLEDGEMENTS

We thank the National Synchrotron Research Center, Thailand and staff for supporting this work. Valuable comments from Dr. Yutaka Sagara on the manuscript are gratefully acknowledged.

FUNDING

This work was partly supported by Mahidol University, Thailand (to J.Y.); and A*STAR, Singapore (to R.C.R.).

CONFLICT OF INTEREST

None declared.

REFERENCES

1. Gould, G.W. (1995) Biodeterioration of foods and an overview of preservation in the food and dairy industries. *Int. Biodeterior. Biodegrad.* **36**, 267–277
2. Kravchenko, N.A. (1967) Lysozyme as a transferase. *Proc. R. Soc. Lond. B Biol. Sci.* **167**, 429–430
3. Fukamizo, T., Goto, S., Torikata, T., and Araki, T. (1989) Enhancement of transglycosylation activity of lysozyme by chemical modification. *Agric. Biol. Chem.* **53**, 2641–2651
4. Blake, C.C., Johnson, L.N., Mair, G.A., North, A.C., Phillips, D.C., and Sarma, V.R. (1967) Crystallographic studies of the activity of hen egg-white lysozyme. *Proc. R. Soc. Lond. B Biol. Sci.* **167**, 378–388
5. Canfield, R.E. (1963) The amino acid sequence of egg white lysozyme. *J. Biol. Chem.* **238**, 2698–2707

6. Jolles, J., Jauregui, A.J., Bernier, I., and Jolles, P. (1963) The chemical structure of hen's egg-white lysozyme: detailed study. *Biochim. Biophys. Acta* **78**, 668–689
7. Blake, C.C., Koenig, D.F., Mair, G.A., North, A.C., Phillips, D.C., and Sarma, V.R. (1965) Structure of hen egg-white lysozyme. A three-dimensional Fourier synthesis at 2 Angstrom resolution. *Nature* **206**, 757–761
8. Grutter, M.G., Rine, K.L., and Matthews, B.W. (1979) Crystallographic data for lysozyme from the egg white of the Embden goose. *J. Mol. Biol.* **135**, 1029–1032
9. Simpson, R.J., Begg, G.S., Dorow, D.S., and Morgan, F.J. (1980) Complete amino acid sequence of the goose-type lysozyme from the egg white of the black swan. *Biochemistry* **19**, 1814–1819
10. Weaver, L.H., Grutter, M.G., Remington, S.J., Gray, T.M., Isaacs, N.W., and Matthews, B.W. (1985) Comparison of goose-type, chicken-type, and phage-type lysozymes illustrates the changes that occur in both amino acid sequence and three-dimensional structure during evolution. *J. Mol. Evol.* **21**, 97–111
11. Inouye, M., Imada, M., and Tsugita, A. (1970) The amino acid sequence of T4 phage lysozyme. IV. Dilute acid hydrolysis and the order of tryptic peptides. *J. Biol. Chem.* **245**, 3479–3484
12. Matthews, B.W. and Remington, S.J. (1974) The three dimensional structure of the lysozyme from bacteriophage T4. *Proc. Natl Acad. Sci. USA* **71**, 4178–4182
13. Lescar, J., Souchon, H., and Alzari, P.M. (1994) Crystal structures of pheasant and guinea fowl egg-white lysozymes. *Protein Sci.* **3**, 788–798
14. Bachali, S., Bailly, X., Jolles, J., Jolles, P., and Deutsch, J.S. (2004) The lysozyme of the starfish Asterias rubens. A paradygmatic type i lysozyme. *Eur. J. Biochem.* **271**, 237–242
15. Gayen, S.K., Som, S., Sinha, N.K., and Sen, A. (1977) Lysozyme in egg whites of tortoises and turtle. Purification and properties of egg white lysozyme of Trionyx gangeticus Cuvier. *Arch. Biochem. Biophys.* **183**, 432–442
16. Aschaffenburg, R., Blake, C.C., Dickie, H.M., Gayen, S.K., Keegan, R., and Sen, A. (1980) The crystal structure of tortoise egg-white lysozyme at 6 Å resolution. *Biochim. Biophys. Acta.* **625**, 64–71
17. Araki, T., Yamamoto, T., and Torikata, T. (1998) Reptile lysozyme: the complete amino acid sequence of soft-shelled turtle lysozyme and its activity. *Biosci. Biotechnol. Biochem.* **62**, 316–324
18. Thammasirirak, S., Ponkham, P., Preecharram, S., Khanchanuan, R., Phonyothee, P., Daduang, S., Srisomsap, C., Araki, T., and Svasti, J. (2006) Purification, characterization and comparison of reptile lysozymes. *Comp. Biochem. Physiol. C Toxicol. Pharmacol.* **143**, 209–217
19. Laemmli, U.K. (1970) Cleavage of structural proteins during the assembly of the head of bacteriophage T4. *Nature* **227**, 680–685
20. Pflugrath, J.W. (1999) The finer things in X-ray diffraction data collection. *Acta Crystallogr.* **D55**, 1718–1725
21. Navaza, J. (1994) AMoRe: an automated package for molecular replacement. *Acta Crystallogr.* **A50**, 157–163
22. Collaborative Computational Project, Number 4 (1994) The CCP4 suite: programs for protein crystallography. *Acta. Crystallogr.* **D50**, 760–763
23. Murshudov, G.N., Vagin, A.A., and Dodson, E.J. (1997) Refinement of macromolecular structures by the maximum-likelihood method. *Acta. Crystallogr.* **D53**, 240–255
24. Jones, T.A., Zou, J.Y., Cowan, S.W., and Kjeldgaard, M. (1991) Improved methods for building protein models in electron density maps and the location of errors in these models. *Acta. Crystallogr.* **A47**, 110–119
25. Laskowski, R.A., MacArthur, M.W., Moss, D.S., and Thornton, J.M. (1993) PROCHECK: a program to check the stereochemical quality of protein structures. *J. Appl. Crystallogr.* **26**, 283–291
26. Thompson, J.D., Higgins, D.G., and Gibson, T.J. (1994) CLUSTAL W: improving the sensitivity of progressive multiple sequence alignment through sequence weighting, position-specific gap penalties and weight matrix choice. *Nucleic Acids Res.* **22**, 4673–4680
27. Gouet, P., Courcelle, E., Stuart, D.I., and Metoz, F. (1999) ESPript: analysis of multiple sequence alignments in PostScript. *Bioinformatics* **15**, 305–308
28. Koradi, R., Billeter, M., and Wuthrich, K. (1996) MOLMOL: a program for display and analysis of macromolecular structures. *J. Mol. Graph.* **14**, 51–55, 29–32
29. Matthews, B.W. (1968) Solvent content of protein crystals. *J. Mol. Biol.* **33**, 491–497
30. Blake, C.C., Pulford, W.C., and Artymiuk, P.J. (1983) X-ray studies of water in crystals of lysozyme. *J. Mol. Biol.* **167**, 693–723
31. Strynadka, N.C. and James, M.N. (1991) Lysozyme revisited: crystallographic evidence for distortion of an *N*-acetylmuramic acid residue bound in site D. *J. Mol. Biol.* **220**, 401–424
32. Cheetham, J.C., Artymiuk, P.J., and Phillips, D.C. (1992) Refinement of an enzyme complex with inhibitor bound at partial occupancy. Hen egg-white lysozyme and tri-*N*-acetylchitotriose at 1.75 Å resolution. *J. Mol. Biol.* **224**, 613–628
33. Hill, C.P., Johnston, N.L., and Cohen, R.E. (1993) Crystal structure of a ubiquitin-dependent degradation substrate: a three-disulfide form of lysozyme. *Proc. Natl. Acad. Sci. USA* **90**, 4136–4140
34. Weisman, L.S., Krummel, B.M., and Wilson, A.C. (1986) Evolutionary shift in the site of cleavage of prelysozyme. *J. Biol. Chem.* **261**, 2309–2313
35. Kawamura, S., Toshima, G., Imoto, T., Araki, T., and Torikata, T. (2002) Amino acid residues in subsites e and f responsible for the characteristic enzymatic activity of duck egg-white lysozyme. *J. Biochem. (Tokyo)* **131**, 663–670
36. Toshima, G., Kawamura, S., Araki, T., and Torikata, T. (2003) Histidine-114 at subsites E and F can explain the characteristic enzymatic activity of guinea hen egg-white lysozyme. *Biosci. Biotechnol. Biochem.* **67**, 540–546
37. Kawamura, S., Eto, M., Imoto, T., Ikemizu, S., Araki, T., and Torikata, T. (2004) Functional and structural effects of mutagenic replacement of Asn37 at subsite F on the lysozyme-catalyzed reaction. *Biosci. Biotechnol. Biochem.* **68**, 593–601